Available online at www.sciencedirect.com
ScienceDirect
Physics Letters B 642 (2006) 100–105
PHYSICS LETTERS B
www.elsevier.com/locate/physletb

A reanalysis of the LSND neutrino oscillation experiment

A. Samana [a,b,c,*], F. Krmpotić [b,d,e], A. Mariano [c,d], R. Zukanovich Funchal [b]

[a] *Centro Brasileiro de Pesquisas Físicas, CEP, 22290-180 Rio de Janeiro, Brazil*
[b] *Instituto de Física, Universidade de São Paulo, C.P. 66.318, 05315-970 São Paulo, Brazil*
[c] *Departamento de Física, Facultad de Ciencias Exactas, Universidad Nacional de La Plata, CP 1900 La Plata, Argentina*
[d] *Instituto de Física La Plata, CONICET, 115 y 49, CP 1900 La Plata, Argentina*
[e] *Facultad de Ciencias Astronómicas y Geofísicas, Universidad Nacional de La Plata, 1900 La Plata, Argentina*

Received 22 August 2005; received in revised form 11 July 2006; accepted 7 August 2006

Available online 20 September 2006

Editor: W. Haxton

Abstract

We reanalyse the LSND neutrino oscillation results in the framework of the projected quasiparticle random phase approximation (PQRPA), which is the only RPA model that treats the Pauli principle correctly, and accounts satisfactorily for great majority of the weak decay observables around ^{12}C. We have found that the employment of the PQRPA inclusive DIF $^{12}\mathrm{C}(\nu_e, e^-)^{12}\mathrm{N}$ cross-section, instead of the CRPA used by the LSND Collaboration in the $\nu_\mu \to \nu_e$ oscillations study of the 1993–1995 data sample, leads to the following: (1) the oscillation probability is increased from $(0.26 \pm 0.10 \pm 0.05)\%$ to $(0.33 \pm 0.10 \pm 0.13)\%$, and (2) the previously found consistence between the $(\sin^2 2\theta, \Delta m^2)$ confidence level regions for the $\nu_\mu \to \nu_e$ and the $\bar{\nu}_\mu \to \bar{\nu}_e$ oscillations is significantly diminished. These effects are not due to the difference in the uncertainty ranges for the neutrino–nucleus cross-section, but to the difference in the cross-sections themselves.

PACS: 14.60.Pq; 23.40.Bw

Several recent experiments [1–7] strongly suggest that neutrinos oscillate. This means that a neutrino of a certain flavor (e.g. ν_μ) transforms as it propagates into a neutrino of another flavor (e.g. ν_e), violating the conservation of the lepton number. For this to happen, the simplest and most widely accepted explanation is that neutrinos have masses and mixing. There are evidences of transitions for three different Δm^2: $\sim 8 \times 10^{-5}$ eV^2 (solar), $\sim 2.5 \times 10^{-3}$ eV^2 (atmospheric) and ~ 1 eV^2 (LNSD), which cannot all be understood in the context of three neutrino oscillations. Normally, the *liquid scintillator neutrino detector* (LSND) results are not taken into account when fitting neutrino oscillation data. Nevertheless, one has to try to understand the real significance of the LSND measurements, specially because $\Delta m^2 \sim 1$ eV^2 is of particular interest to astrophysics and cosmology. The LSND experiment took place over six calendar years finding evidence for the appearance of electron–antineutrinos $\bar{\nu}_e$ at the 3.3σ level [1,3], and at lesser significance they have observed as well hints for the appearance of electron–neutrinos ν_e [2,3]. The first of these signals is the main LSND result and the second weaker signal was used as a consistency check. The positive results in both channels were interpreted in a two-flavor framework as transitions between the weak eigenstates ν_μ ($\bar{\nu}_\mu$) and ν_e ($\bar{\nu}_e$) driven by masses and mixing. In fact, quantum mechanics dictates that in this case the normally observed weak eigenstates (ν_μ, ν_e) can oscillate between each other with probability

$$P_{\nu_\mu \to \nu_e} = \sin^2(2\theta) \sin^2\left(1.27 \Delta m^2 \frac{L_\nu}{E_\nu}\right), \tag{1}$$

if they are composed of a mixture of mass eigenstates (ν_1, ν_2). Here θ is the mixing angle between the mass and flavor bases, $\Delta m^2 = m_1^2 - m_2^2$ is the ν_1 and ν_2 mass squared differences in eV^2, L_ν is the baseline, the distance in meters travelled by the neutrino from the source to the detector, and E_ν is the neutrino energy in MeV.

The combination of the LSND data with other compelling evidences for neutrino oscillations, stemming from atmospher-

* Corresponding author.
E-mail address: arturo@cbpf.br (A. Samana).

0370-2693/$ – see front matter
doi:10.1016/j.physletb.2006.08.071

ic [4], solar [5], KamLAND [6] reactor, and K2K [7] accelerator neutrino experiments, cannot be adequately explained in the standard three-neutrino picture with *CPT* conservation, and this issue is considered to be a big challenge for neutrino phenomenology [8–10]. Models with four light neutrinos (the extra neutrino being sterile) [11] or *CPT* violation [12] with three neutrinos have been proposed to accommodate all neutrino data. However, in both cases, recent analyses show that neither scenario provides a satisfactory description of the data [13,14].

In the LSND experiment the neutrinos ν_μ come from the decay of π^+ in flight (*decay in flight*, DIF), whereas the neutrinos ν_e and the antineutrinos $\bar{\nu}_\mu$ come from the decay of μ^+ at rest (*decay at rest*, DAR), i.e.,

$$\begin{array}{ll} \pi^+ \to \mu^+ + \nu_\mu & \pi^+ \to \mu^+ + \nu_\mu \\ & \quad\downarrow \\ & \quad e^+ + \nu_e + \bar{\nu}_\mu \\ \text{DIF} & \quad\text{DAR} \end{array}$$

The search for the DAR $\bar{\nu}_\mu \to \bar{\nu}_e$ oscillations [1,3] involves the measurement of the reaction $p(\bar{\nu}_e, e^+)n$, which has a large and well-known cross-section. The events are identified by detecting both the e^+ and the 2.2 MeV γ-ray from the reaction $p(n,\gamma)d$. On the other hand, the signature for the DIF $\nu_\mu \to \nu_e$ oscillations [2,3] is marked by the presence of an isolated high energy electron ($60 < E_e^{\rm DIF} < 200$ MeV) in the detector. It is produced by the charge-exchange reaction $^{12}{\rm C}(\nu_e, e^-)^{12}{\rm N}$, which takes place throughout the tank, the cross-section of which σ_e is, as yet, not well established. The lower and upper energy cuts for $E_e^{\rm DIF}$ were chosen in such a way as to be above the Michel electron end point of 52.8 MeV and below the point where the beam-off background starts to increase rapidly and the signal becomes negligible.

There are two LSND studies of the DIF $\nu_\mu \to \nu_e$ oscillations. The first analysis was done on the 1993–1995 data sample [2], which gave a total of $N_{\nu_e}^{\rm osc} = 18.1 \pm 6.6 \pm 4.0$ oscillation events, corresponding to a transition probability

$$P_{\nu_\mu \to \nu_e}^{\rm exp} = (2.6 \pm 1.0 \pm 0.5) \times 10^{-3}, \tag{2}$$

when the cross-section σ_e predicted by Kolbe et al. within the continuum random phase approximation (CRPA) is used [15]. In the second search, the 1996–1998 data sample [3] was included as well, with reduced DIF flux and higher beam-off background compared to the 1993–1995 data. The reason for this modification lies in the fact that in this study first priority was given to the DAR $\bar{\nu}_\mu \to \bar{\nu}_e$ oscillations, which have been analysed jointly. Moreover, for σ_e has been employed in this occasion two different models. Namely, the shell model (SM) estimate, done by Hayes and Towner [16], for the DAR region, and a relativistic Fermi gas model for the DIF region. The resulting total excess was $N_{\nu_e}^{\rm osc} = 8.1 \pm 12.2 \pm 1.7$ events, yielding

$$P_{\nu_\mu \to \nu_e}^{\rm exp} = (1.0 \pm 1.6 \pm 0.4) \times 10^{-3}. \tag{3}$$

The aim of the present work is to explore the role played by these nuclear structure effects in the delimitation of the neutrino parameters for the DIF $\nu_\mu \to \nu_e$ oscillations.[1]

Before proceeding, and to make more clear the objective of the present work, it is convenient to discuss briefly the flux-averaged exclusive cross-sections

$$\bar{\sigma}_\ell^{\rm exc} = \int_0^{E_{\nu_\ell}^{\max}} dE_\nu\, \sigma_\ell\big(E_\ell = E_\nu - \Delta, 1_1^+\big)\Phi_\ell(E_\nu) \tag{4}$$

and the inclusive cross-sections

$$\bar{\sigma}_\ell^{\rm inc} = \int_0^{E_{\nu_\ell}^{\max}} dE_\nu\, \sigma_\ell(E_\nu)\Phi_\ell(E_\nu), \tag{5}$$

where

$$\sigma_\ell(E_\nu) = \sum_{J_f^\pi} \sigma_\ell\big(E_\ell = E_\nu - \omega_{J_f^\pi}, J_f^\pi\big); \quad \ell = e, \mu. \tag{6}$$

The spin and parity-dependent cross-section $\sigma_\ell(E_\ell, J_f^\pi)$ is given by [17, (2.19)], ω_{J_f} are the excitation energies in ^{12}N relative to the ground state in ^{12}C, and $\Delta \equiv \omega_{1_1^+} = 17.3$ MeV. The energy integration for electrons is carried out in the DAR interval $m_e + \omega_{J_f} \leqslant \Delta_{J_f}^{\rm DAR} \leqslant E_{\nu_e}^{\max} = 52.8$ MeV, and for muons in the DIF interval up to $m_\mu + \omega_{J_f} \leqslant \Delta_{J_f}^{\rm DIF} \leqslant E_{\nu_\mu}^{\max} = 300$ MeV.[2] $\Phi_\ell(E_\nu)$ is the normalised neutrino flux; for ν_e it is approximated by the Michel spectrum, and for ν_μ that from Ref. [18] was used.

The experimental data for the exclusive and inclusive cross-sections, given in Table 1, show that the DAR and DIF processes are of quite different nature: while the first one is dominated in proportion of 2/3 by the Gamow–Teller (GT) transition to the ground state 1_1^+ in ^{12}N, the second one populates almost entirely the excited states through the forbidden transitions. It is quite a difficult task for the nuclear structure models to describe both cross-sections simultaneously.

The SM treats correctly the Pauli principle within the p-shell, which is crucial for the correct distribution of the GT strength, whereas the predictions for high-lying states are less certain because of the truncation of the model space. In fact, the SM calculation performed by Hayes and Towner [16] reproduces fairly well several data. But, in a later SM study, Volpe et al. [19] noted that this concordance could be an artifact because the employed model space was not large enough to exhaust the charge-exchange sum rules. More, the same authors have shown that when a more extended space is employed the SM cross-sections are increased exceeding the experimental LSND result.

[1] Accurate knowledge of the ν cross-section, and the related observables, plays an important role for the next generation of experiments. Various target nuclei, like C, O, Fe, Ar, Pb, ..., are normally (and presumably will be) employed to provide the detector mass.

[2] In order to invert the summation on J_f^π and the integration on dE_ν, we have extended the lower limit of integration in (4) from $m_\ell + \omega_{J_f}$ to zero by defining $\sigma_\ell(E_\ell = E_\nu - \omega_{J_f}, J_f^\pi) \equiv 0$ for $E_\ell < m_\ell$.

Table 1
Calculated and experimental flux-averaged exclusive $\bar{\sigma}^{\rm exc}_{e,\mu}$, and inclusive $\bar{\sigma}^{\rm inc}_{\mu}$ cross-section for the ^{12}C$(\nu_e, e^-)^{12}$N DAR reaction (in units of 10^{-42} cm^2) and for the ^{12}C$(\nu_\mu, \mu^-)^{12}$N DIF reaction (in units of 10^{-40} cm^2). The CRPA calculations [15] were used in the first LSND analysis on the 1993–1995 data sample [2], and the SM calculations from Ref. [16] in the second LSND oscillation search [3]. The listed PQRPA results correspond to the calculations performed with the relativistic corrections included [17]. One alternative SM result as well as the RPA and QRPA results from Ref. [19] are also shown

	$\bar{\sigma}^{\rm exc}_{e}$	$\bar{\sigma}^{\rm inc}_{e}$	$\bar{\sigma}^{\rm exc}_{\mu}$	$\bar{\sigma}^{\rm inc}_{\mu}$
Theory				
CRPA [15]	36.0, 38.4	42.3, 44.3	2.48, 3.11	21.1, 22.8
SM [16]	7.9	12.0	0.56	13.8
PQRPA [17]	8.1	18.6	0.59	13.0
SM [19]	8.4	16.4	0.70	21.1
RPA [19]	49.5	55.1	2.09	19.2
QRPA [19]	42.9	52.0	1.97	20.3
Experiment				
Ref. [20]	$9.1 \pm 0.4 \pm 0.9$	$14.8 \pm 0.7 \pm 1.4$		
Ref. [21]			$0.66 \pm 0.1 \pm 0.1$	$12.4 \pm 0.3 \pm 1.8$
Ref. [22]	$8.9 \pm 0.3 \pm 0.9$	$13.2 \pm 0.4 \pm 0.6$		
Ref. [23]			$0.56 \pm 0.08 \pm 0.10$	$10.6 \pm 0.3 \pm 1.8$

The RPA like models include high-lying one-particle one-hole excitations, but very frequently completely fail to account for the amount and distribution of the GT strength as can be seen from Table 1. This is the reason why the CRPA is unable to explain the weak processes (β-decays, μ-capture, and neutrino induced reactions) among the ground states of the triad $\{^{12}$B, ^{12}C, ^{12}N$\}$: a rescaling factor of the order of 4 is needed to bring the calculations and the data to agree [15], and a subsequent ad hoc inclusion of partial occupancy of the $p_{1/2}$ subshell reduces this factor to less than 2 [24,25]. It is still more relevant here that the CRPA overestimates the inclusive ^{12}C$(\nu_\mu, \mu^-)^{12}$N cross-section with ν_μ coming from the DIF of π^+ by about 50% [21] or more [23], because one can assume that the DIF ^{12}C$(\nu_e, e^-)^{12}$N cross-section, which gauges the $\nu_\mu \to \nu_e$ oscillations, is affected in the same proportion. This assumption comes from the universality of the weak interaction and was done in the first LSND analysis [2].[3]

Thus, it might be interesting to reanalyse the LSND results in the framework of the projected quasiparticle random phase approximation (PQRPA) [27], which is the only RPA model that treats correctly the Pauli principle, explaining in this way the distribution of the GT strength. To achieve this it was imperative both: (a) to include the BCS correlations, and (b) to perform the particle number projection. Under these conditions most of the weak decay observables around ^{12}C are within 20% of the PQRPA predictions. This happens, for instance, with: (1) the B(GT)-values to ^{12}N and ^{12}B, (2) the exclusive muon captures to the 1^+_1, 2^+_1, 1^-_1 and 2^-_1 states, as well as the inclusive muon capture in ^{12}B, and (3) the exclusive cross-sections $\bar{\sigma}^{\rm exc}_e$ and $\bar{\sigma}^{\rm exc}_\mu$ and the inclusive cross-section $\bar{\sigma}^{\rm exc}_\mu$ [17,27]. The only exception is the inclusive cross-section, $\bar{\sigma}^{\rm inc*}_e = \bar{\sigma}^{\rm inc}_e - \bar{\sigma}^{\rm exc}_e$, for which the PQRPA value, 10.5 (in units of 10^{-40} cm^2), is more than 100% larger that the experiment result, $4.3 \pm 0.4 \pm 0.6$ [22]. From the nuclear structure point of view the theoretical evaluation of this quantity is a peculiarly delicate and subtle issue and therefore deserves a special comment. In fact from Table VI in Ref. [17] it can be seen that in the PQRPA case $\bar{\sigma}^{\rm inc*}_e$ is build up from the interplay of GT strength not contained in the 1^+_1 state, the Fermi (F) transitions to the 0^+ states, and the first forbidden transitions to the 1^- and 2^- states. All these quantities are relatively small and evaluating them precisely is a very difficult task. Then one should not be surprised by the most recent SM calculation [19] which yields a result ($\bar{\sigma}^{\rm inc*}_e = 8.3$) which is twice as large as that obtained in the previous SM study: $\bar{\sigma}^{\rm inc*}_e = 4.1$ [16]. The CRPA result $\bar{\sigma}^{\rm inc*}_e = 6.3$ [15], very likely does not contain any GT and F strengths as it should, and therefore, in this case, the agreement with the experiment could be accidental.

We will limit our attention only to the 1993–1995 data sample [2], which, as mentioned before, yields a more defined signal for the oscillation events. The experimental oscillation probability can be written as

$$P^{\rm exp}_{\nu_\mu \to \nu_e} = \frac{N_\nu}{\epsilon f_n \langle \sigma \Phi_{\nu_\mu} \rangle} - \frac{\langle \sigma \Phi_{\nu_e} \rangle}{\langle \sigma \Phi_{\nu_\mu} \rangle}, \tag{7}$$

where the ν_e flux (from now on) is defined as

$$\Phi_{\nu_e} = \Phi^{\mu^+}_{\nu_e} + \Phi^{\pi^+}_{\nu_e}, \tag{8}$$

with the fluxes $\Phi^{\mu^+}_{\nu_e}$ and $\Phi^{\pi^+}_{\nu_e}$ coming, respectively, from the DIF decays $\pi^+ \to e^+ + \nu_e$ and $\mu^+ \to e^+ + \nu_e + \bar{\nu}_\mu$. $f_n = (9.23 \times 10^{22}) \cdot (5.4 \times 10^{30})$, with the first quantity being the number of protons on target (POT), while the second one is the fiducial volume (number of molecules of CH_2 in the detector tank). $N_\nu = N^{\rm osc}_\nu + N^{\rm bg}_\nu = 27.7 \pm 6.9$ is the total number of beam-excess events measured by LSND, and ϵ is the event selection efficiency. The averaged inclusive cross-sections are

$$\langle \sigma \Phi_{\nu_\ell} \rangle = \sum_{J^\pi_f} \int_{E^<_{J^\pi_f}}^{E^>_{J^\pi_f}} \sigma_e\big(E_e = E_\nu - \omega_{J_f}, J^\pi_f\big) \Phi_{\nu_\ell} \, dE_\nu;$$
$$\ell = e, \mu, \tag{9}$$

[3] Since the work of O'Connell, Donelly and Walecka [26] we know that electron and muon cross-sections differ for low neutrino energy, but tend to merge for high neutrino energy.

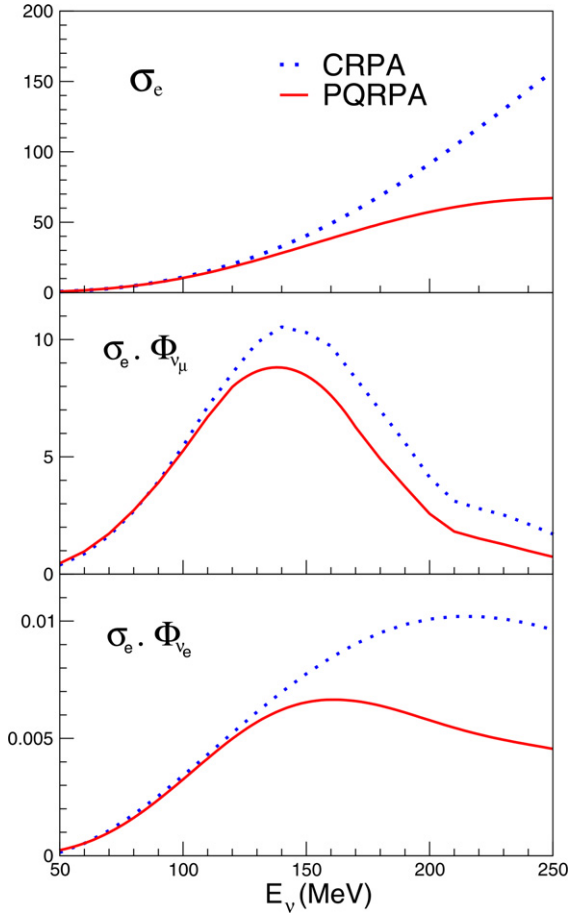

Fig. 1. (Colour online.) Comparison between the CRPA and PQRPA results for: $\sigma_e(E_\nu)$ in units of 10^{-40} cm^2 (upper panel), and, in units of 10^{-52} POT^{-1} MeV^{-1}, for $\sigma_e(E_\nu)\Phi_{\nu_\mu}$ (middle panel) and $\sigma_e(E_\nu)\Phi_{\nu_e}$ (lower panel).

where $E^<_{J^\pi_f} = 60$ MeV $+ \omega_{J^\pi_f}$ and $E^>_{J^\pi_f} = 200$ MeV $+ \omega_{J^\pi_f}$. In order to simplify the numerical calculations which follow, instead of using the exact equations (8), we will employ here the approximate ones:

$$\langle \sigma \Phi_{\nu_\ell} \rangle = \int_{E^<}^{E^>} \sigma_e(E_\nu)\Phi_{\nu_\ell}\, dE_\nu; \quad \ell = e, \mu, \tag{10}$$

where $\sigma_e(E_\nu)$ is given by (5), and $E^< = 60$ MeV $+ \Delta$, and $E^> = 200$ MeV $+ \Delta$. We have verified numerically that Eqs. (10) reproduce Eqs. (9) up to a few per cent. The neutrino fluxes Φ_{ν_μ}, $\Phi^{\pi^+}_{\nu_e}$ and $\Phi^{\mu^+}_{\nu_e}$ were adopted from Ref. [2]. The CRPA and PQRPA results for $\sigma_e(E_\nu)$, $\sigma_e(E_\nu)\Phi_{\nu_\mu}$ and $\sigma_e(E_\nu)\Phi_{\nu_e}$ are confronted in Fig. 1, as a function of E_ν.

The systematic error associated with the PQRPA cross-section is taken to be 20%, based on our theoretical uncertainties (see Tables V–VII in [17]), and agreement between measured data and theoretical predictions for the weak decay observables involving the ^{12}C nucleus [17,27]. Therefore, considering the same uncertainties as in the LSND search [2] in the selection of ϵ (12%) and in the flux Φ_{ν_μ} (15%), we end up with a total systematic error of 28%, which yields $N^{\rm osc}_\nu = 21.5 \pm 6.6 \pm 8.5$. In this way the PQRPA result for the oscillation probability turns out to be:

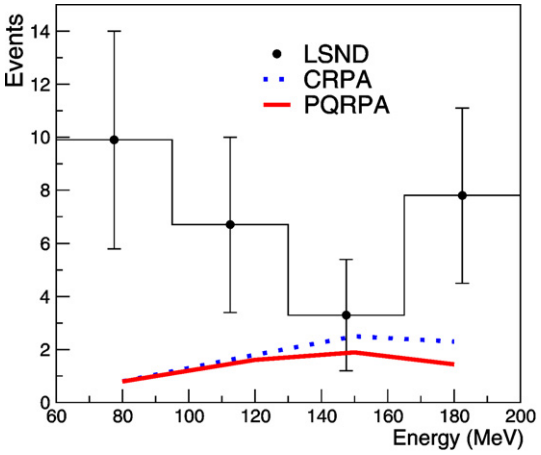

Fig. 2. (Colour online.) The energy distribution (in 4 energy bins) of the LNSD excess events, $N_\nu(i)$, together with the corresponding experimental errors $\delta N_\nu(i)$ (vertical lines) and the energy intervals $E_\nu(i)$ (horizontal lines). The theoretical CRPA and PQRPA values for the expected background events, $\tilde{N}^{\rm bg}_\nu(i)$, are shown as well.

$$P^{\rm exp}_{\nu_\mu \to \nu_e} = (3.3 \pm 1.0 \pm 1.3) \times 10^{-3}. \tag{11}$$

The difference when compared to the CRPA result (2) is due to the difference in the electron cross-section, as evidenced in Fig. 1.

In order to determine a confidence region in the $(\sin^2 2\theta, \Delta m^2)$ parameter space we proceed in the same manner as in Ref. [2]. First we rearrange the data for energy distribution of the excess events (see [2, Fig. 29]) in four equal energy bins $N_\nu(i)$, as shown in Fig. 2. Next, we minimise the χ^2 function

$$\chi^2 = \sum_{i=1}^{4} \left[\frac{N_\nu(i) - \tilde{N}_\nu(i)}{\delta N_\nu(i)} \right]^2, \tag{12}$$

where $\tilde{N}_\nu(i) = \tilde{N}^{\rm osc}_\nu(i) + \tilde{N}^{\rm bg}_\nu(i)$, with

$$\begin{aligned} \tilde{N}^{\rm osc}_\nu(i) &= \epsilon f_n \int_{E_\nu(i)} \sigma(E_\nu)\mathcal{R}(E_\nu)\Phi_{\nu_\mu}(E_\nu) P_{\nu_\mu \to \nu_e}\, dE_\nu, \\ \tilde{N}^{\rm bg}_\nu(i) &= \epsilon f_n \int_{E_\nu(i)} \sigma(E_\nu)\mathcal{R}(E_\nu)\Phi^{\rm bg}_{\nu_e}(E_\nu)\, dE_\nu, \end{aligned} \tag{13}$$

where $P_{\nu_\mu \to \nu_e}$ is a function of E_ν, $\sin^2(2\theta)$ and Δm^2, and is defined in (1). We include the resolution function [28],

$$\mathcal{R}(E_\nu) = \frac{1}{\sqrt{2\pi}\varepsilon(E_\nu)} \int_{E_<}^{E_>} \exp\left[-\frac{1}{2} \left(\frac{E'_\nu - E_\nu}{\varepsilon(E_\nu)} \right)^2 \right] dE'_\nu, \tag{14}$$

which takes into account the probability for finding the electron inside the window of detection, with $\varepsilon(E_\nu) = 0.06 E_\nu$ being the experimental energy resolution [2].

To set the confidence levels (CL) we used the raster scan method [29]: for each value of Δm^2, a best fit is found for $\sin^2 2\theta$. At each Δm^2, χ^2 is calculated as a function of $\sin^2 2\theta$. The 1D confidence interval in $\sin^2 2\theta$ at Δm^2 is composed of all points having a χ^2 within 3.84 of the minimum value (3.84

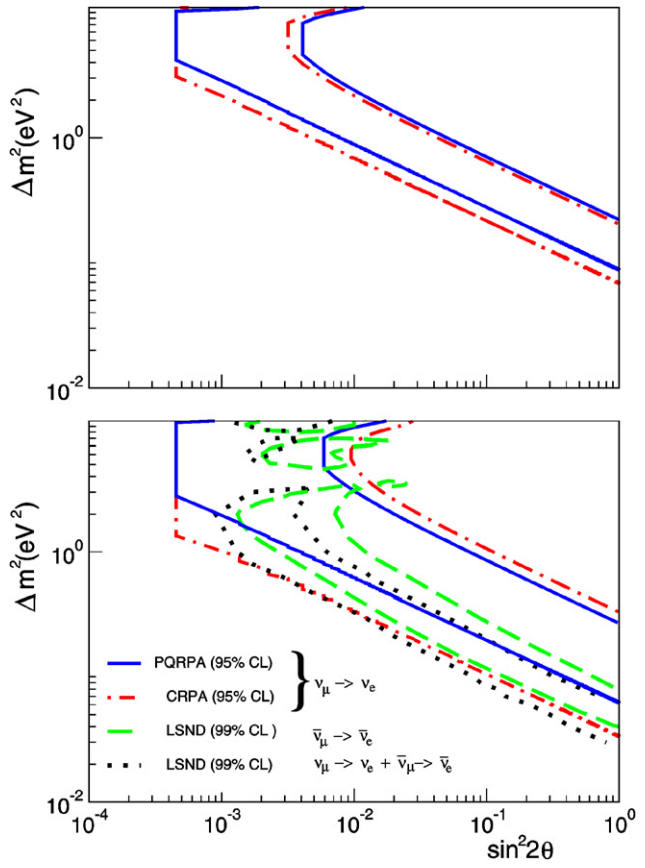

Fig. 3. (Colour online.) Regions in the neutrino oscillation parameter space. In the upper panel the results for $\nu_\mu \to \nu_e$ oscillations without the inclusion of the systematic uncertainty are shown, while the lower panel shows those with the uncertainty included, as described in the text.

is the two-sided 95% CL for a distribution χ^2 with one degree of freedom). The confidence region in the $(\sin^2 2\theta, \Delta m^2)$ is the union of all these intervals.

Our $(\sin^2 2\theta, \Delta m^2)$ oscillation parameter fits for the DIF channel $\nu_\mu \to \nu_e$, corresponding to both the CRPA [15] and PQRPA [17] cross-sections, are shown in Fig. 3, along with the favoured regions for the LSND DAR measurement for $\bar{\nu}_\mu \to \bar{\nu}_e$ [1]. In order to better understand the consequences of using different cross-sections, the confidence regions obtained with (lower panel) and without (upper panel) inclusion of the systematic uncertainties, are displayed separately. In the calculation with the CRPA cross-section these uncertainties are taken to be the same as in the LSND search [2], i.e., of 22% for the positive side, which shifts the parameter space downwards, and of 45% for the negative side, which shifts the parameter space upwards. On the other hand, an uncertainty of 28% is used for both negative and positive side, when the PQRPA cross-section is employed.

We see that, when the systematic uncertainties are considered, the CRPA 95% CL region fully comprises the 99% CL region for the $\bar{\nu}_\mu \to \bar{\nu}_e$ oscillations, which is in essence the result obtained by the LSND Collaboration [2]. Contrarily, this does not happen in the PQRPA case where the overlapping between the two regions is only marginal. It is important to stress that the $\nu_\mu \to \nu_e$ region is dragged towards the $\bar{\nu}_\mu \to \bar{\nu}_e$ region by the positive side uncertainty, while the role played by the negative side uncertainty is of minor importance. For the sake of completeness the result of the joint $\nu_\mu \to \nu_e$ and $\bar{\nu}_\mu \to \bar{\nu}_e$ oscillation parameter fit over $(\sin^2 2\theta, \Delta m^2)$ plane for the complete 1993–1998 data sample [3], is also displayed in Fig. 3.

In summary, we have found that the employment of a smaller inclusive DIF $^{12}\mathrm{C}(\nu_e, e^-)^{12}\mathrm{N}$ cross-section, than the one used by the LSND Collaboration [2] in the $\nu_\mu \to \nu_e$ oscillations study of the 1993–1995 data sample, leads to the following consequences: (1) the oscillation probability $P^{\mathrm{exp}}_{\nu_\mu \to \nu_e}$ is increased, and (2) the previously found consistence between the $(\sin^2 2\theta, \Delta m^2)$ confidence level regions for the $\nu_\mu \to \nu_e$ and the $\bar{\nu}_\mu \to \bar{\nu}_e$ oscillations is diminished. More, these effects are not due to the difference in the uncertainty ranges for the neutrino–nucleus cross-section, but to the difference in the cross-sections themselves, and are quite significant when the PQRPA is used instead of the CRPA. Thus, precise knowledge of the nuclear structure involved in the ν-nucleus cross-section, could play an important role in the delimitation of the neutrino parameters for the DIF $\nu_\mu \to \nu_e$ oscillations.

Acknowledgements

F.K. and A.M. are fellows of the CONICET, Argentina. A.S. acknowledges support received from Conselho Nacional de Ciência e Tecnologia (CNPq) and Fundação de Amparo à Pesquisa do Estado do Rio de Janeiro (FAPERJ). R.Z.F. thanks CNPq and Fundação de Amparo à Pesquisa do Estado de São Paulo (FAPESP) for partial financial support. We are extremely grateful to Gordana Tadić for her very careful reading of the manuscript.

References

[1] C. Athanassopoulos, et al., LSND Collaboration, Phys. Rev. C 54 (1996) 2685;
C. Athanassopoulos, et al., LSND Collaboration, Phys. Rev. Lett. 77 (1996) 3082.
[2] C. Athanassopoulus, et al., LSND Collaboration, Phys. Rev. C 58 (1998) 2489;
C. Athanassopoulus, et al., LSND Collaboration, Phys. Rev. Lett. 81 (1998) 1774.
[3] A. Aguilar, et al., LSND Collaboration Phys. Rev. D 64 (2001) 112007, hep-ex/0104049.
[4] Y. Fukuda, et al., Super-Kamiokande Collaboration, Phys. Rev. Lett. 81 (1998) 1562;
Y. Ashie, et al., Super-Kamiokande Collaboration, Phys. Rev. Lett. 93 (2004) 101801, hep-ex/0501064.
[5] B. Aharmim, et al., SNO Collaboration, hep-ex/0502021;
M.B. Smy, et al., Super-Kamiokande Collaboration, Phys. Rev. D 69 (2004) 011104;
C. Cattadori, Results from Radiochemical Solar Neutrino Experiments, XXIth International Conference on Neutrino Physics and Astrophysics (Neutrino 2004), Paris, 14–19 June 2004.
[6] T. Araki, et al., KamLAND Collaboration, Phys. Rev. Lett. 94 (2005) 081801, hep-ex/0406035.
[7] M.H. Ahn, et al., K2K Collaboration, Phys. Rev. Lett. 90 (2003) 041801.
[8] T. Schwetz, hep-ph/0311217, and references therein.
[9] M. Maltoni, T. Schwetz, M. Tórtola, J.W.F. Valle, New J. Phys. 6 (2004) 122.
[10] Y. Fukuda, et al., Phys. Lett. B 335 (1994) 237.

[11] For a discussion and an extensive bibliography see V. Barger, D. Marfatia, K. Whisnant, Int. J. Mod. Phys. E 12 (2003) 569, hep-ph/0308123.
[12] H. Murayama, T. Yanagida, Phys. Lett. B 520 (2001) 263, hep-ph/0010178;
G. Barenboim, L. Borissov, J. Lykken, A.Y. Smirnov, JHEP 0210 (2002) 001, hep-ph/0108199;
G. Barenboim, L. Borissov, J. Lykken, Phys. Lett. B 534 (2002) 106, hep-ph/0201080.
[13] M. Maltoni, T. Schwetz, M. Tórtola, J.W.F. Valle, Nucl. Phys. B 643 (2002) 321, hep-ph/0207157.
[14] A. Strumia, Phys. Lett. B 539 (2002) 91, hep-ph/0201134;
M.C. Gonzalez-Garcia, M. Maltoni, T. Schwetz, Phys. Rev. D 68 (2003) 053007, hep-ph/0306226.
[15] E. Kolbe, K. Langanke, S. Krewald, Phys. Rev. C 49 (1994) 1122.
[16] A.C. Hayes, I.S. Towner, Phys. Rev. C 61 (2000) 044603.
[17] F. Krmpotić, A. Mariano, A. Samana, Phys. Rev. C 71 (2005) 044319.
[18] LSND home page, http://www.nu.to.infn.it/exp/all/lsnd/.
[19] C. Volpe, N. Auerbach, G. Colò, T. Suzuki, N. Van Giai, Phys. Rev. C 62 (2000) 015501.
[20] C. Athanassopoulus, et al., LSND Collaboration, Phys. Rev. C 55 (1997) 2078.
[21] C. Athanassopoulus, et al., LSND Collaboration, Phys. Rev. C 56 (1997) 2806.
[22] L.B. Auerbach, et al., LSND Collaboration, Phys. Rev. C 64 (2001) 065501.
[23] L.B. Auerbach, et al., LSND Collaboration Phys. Rev. C 66 (2002) 015501.
[24] N. Auerbach, N. Van Giai, O.K. Vorov, Phys. Rev. C 56 (1997) 2368.
[25] E. Kolbe, K. Langanke, P. Vogel, Nucl. Phys. A 652 (1999) 91.
[26] J.S. O'Connell, T.W. Donelly, J.D. Walecka, Phys. Rev. 6 (1972) 719.
[27] F. Krmpotić, A. Mariano, A. Samana, Phys. Lett. B 541 (2002) 298.
[28] J.N. Bahcall, P.I. Krastev, E. Lisi, Phys. Rev. C 55 (1997) 494.
[29] G. Feldman, R. Cousins, Phys. Rev. D 57 (1998) 3873.